SPE-189783-MS

Material Balance Forecast of Huff-and-Puff Gas Injection in Multiporosity Shale Oil Reservoirs

Daniel Orozco and Roberto Aguilera, Schulich School of Engineering, University of Calgary; Karthik Selvan, Nexen Energy ULC

This paper was prepared for presentation at the SPE Canada Unconventional Resources Conference held in Calgary, Alberta, Canada, 13-14 March 2018.

Abstract

Primary oil recovery from shales is very low, rarely exceeding 10% of original oil in place (OOIP). The low recovery has aroused a recent and growing interest in the petroleum industry for using Improved Oil Recovery (IOR) methods in shales. This paper presents a new semi-analytical material balance equation (MBE) to forecast the performance of shale oil reservoirs under natural depletion and huff-and-puff gas injection scenarios.

For undersaturated reservoirs, recovery is calculated from the proposed MBE explicitly using a multiporosity effective oil compressibility. For saturated reservoirs, the MBE is solved at each pressure step using a finite differences scheme. For huff-and-puff gas injection, the average reservoir pressure p is calculated after injecting a certain gas volume during the huff period. At each huff-and-puff cycle, the remaining OOIP is considered, and the injected gas volume (which is known) is written in terms of the p following injection (which is unknown). Adding the gas injection term to the MBE generates a nonlinear equation for p, which is solved using a numerical method.

Results indicate that oil recovery from shales can be increased significantly by huff-and-puff gas injection. A case study from the Eagle Ford shale in the United States is used to demonstrate these results, which are presented in tabular form as well as crossplots of oil rates, cumulative oil production, gas-oil ratio and average reservoir pressure vs. time. An important feature of the proposed MBE is the inclusion of hydraulic fractures, as well as inorganic, organic and natural fracture porosities. These porosities are included in a history-matching presented in detail for a well undergoing huff-and-puff gas injection.

The novelty of this work resides on the introduction of a new MBE that considers multiple porosities and enables quick evaluations of primary recovery and huff-and-puff gas injection scenarios in shale oil reservoirs. The new MBE results compare favorably against real data of the Eagle Ford shale. The good comparison allows making reasonable projections of future oil rates and cumulative oil recoveries by huff-and-puff gas injection.

Introduction

Exploitation of shale reservoirs has transformed the energy landscape of US and Canada. Despite the outstanding growth of liquids production from shales during the last few years, oil recoveries as a fraction of OOIP remain low and rarely exceed 10%. Further actions beyond the traditional approaches deployed so far by the industry (horizontal wellbores + multistage hydraulic fracturing) are required to improve oil recoveries. As a result, research interest on application of Improved Oil Recovery/Enhanced Oil Recovery (IOR/EOR) methods has arisen during the last two years. At present, both academia and industry are investigating the possibility of implementing IOR and EOR methods in shale reservoirs. The techniques under study include waterflooding (Hoffman and Evans, 2016); huff-and-puff gas injection (Gamadi et al., 2014; Fragoso, 2016); surfactants for reduction of interfacial tension (Rassenfoss, 2017a); and thermal stimulation by means of electromagnetic downhole heating (Egboga et al., 2017). This paper focuses on the effects of huff-and-puff gas injection on oil recovery from shale reservoirs.

Numerical simulation studies by Fragoso et al. (2018a) suggest that huff-and-puff injection of natural gas into the oil container of the Eagle Ford shale has the potential to add 20% to the recovery of liquids. The authors also consider the effects of continuous gas injection, but conclude from both technical and economic standpoints that this scheme does not offer better results if compared to huff-and-puff gas injection schedules. For that reason, our study only devotes its attention to the effects of huff-and-puff gas injection.

Though there is no universal consensus on whether IOR and EOR methods may work in shales, optimism arose recently when EOG Resources, an oil and gas company based in the US, indicated in May 2016 that the first economically successful huff-and-puff gas injection pilots had been conducted in the Eagle Ford shale (Jacobs, 2016). Technical details of the pilots remain confidential, but executives of the company indicated that the rate-of-return (ROR) of the project is comparable to the ROR achieved by drilling a new horizontal well. Furthermore, they indicated that the EOR program offers twice the net present value (NPV) per each dollar spent, and that the 2016 EOR net oil production attained a 70% year-on-year increase. Figure 1 reflects the improvement in oil recoveries claimed by the company. At the time of this publication, and to the best of the authors' knowledge, at least four more major oil companies were planning gas injection pilots in shales both in the US and Canada.

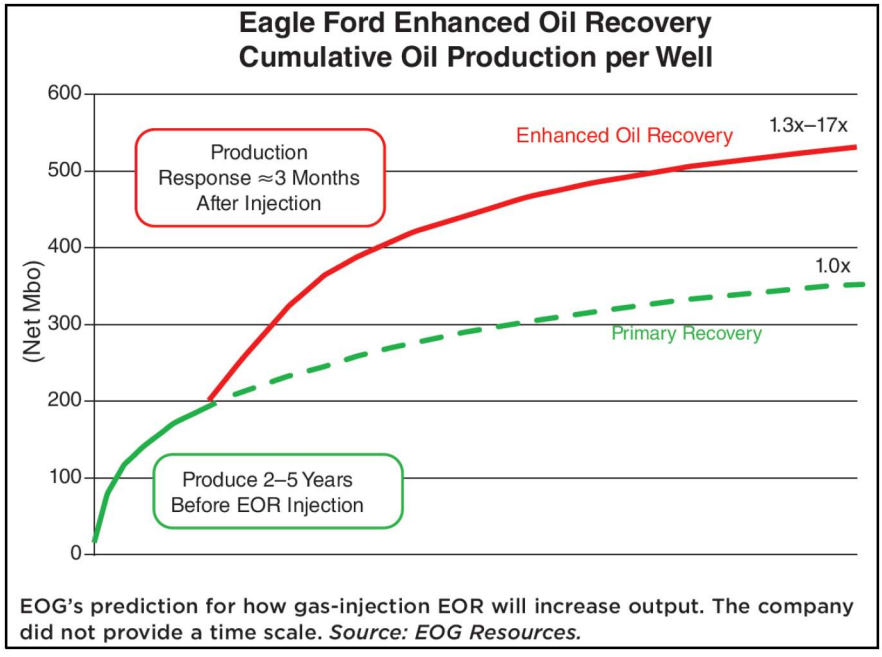

Figure 1—EOG Resources prediction for gas injection EOR in the Eagle Ford (Rassenfoss, 2017b).

So far, the studies supporting the feasibility of huff-and-puff gas injection in shales have relied mostly on detailed, compositional numerical simulation models and some laboratory work. The numerical models are computationally expensive and time-consuming mainly because of their compositional nature and the standard practice of using dual permeability and local grid refinement within the hydraulic fractures.

To alleviate the time-consuming nature of numerical simulation, this study introduces a new semi-analytical MBE to forecast the performance of shale oil reservoirs under natural depletion and huff-and- puff gas injection scenarios. Results are presented as plots of oil rate, cumulative oil recovery, gas-oil ratio and average reservoir pressure vs. time. The methodology is not meant to replace detailed numerical simulation studies, but rather to provide the reservoir engineer with a practical tool for quick estimates of oil recoveries from shale reservoirs performing under primary recovery and huff-and-puff gas injection.

General Observations Regarding Gas Injection in Shales

Thus far, the only successfully implemented and documented gas injection pilot in shales corresponds to the one performed by EOG Resources in the Eagle Ford. As such, the remarks presented in this section are discussed considering special features of this resource play. An important feature of the Eagle Ford shale is its unconventional fluids distribution, which is exactly the opposite of what is observed in conventional reservoirs: black oil is found in a top container; deeper, and to the south, there is volatile oil and gas condensate in a separate container; and dry gas is found in another separate container at the bottom of the structure, as depicted on Figure 2. This upside-down or inverted position has been contained through geologic time as shown by Ramirez and Aguilera (2016). It has been demonstrated that gas produced from the deepest container can be injected into the oil and condensate containers (Fragoso et al., 2018a, 2018b). This is important as some other shales in the world have similar upside-down characteristics to those of the Eagle Ford (for example, the Duvernay shale in Canada and the Niobrara shale in the United States), which makes them also potential candidates for huff-and-puff gas injection with a view to improve oil recoveries.

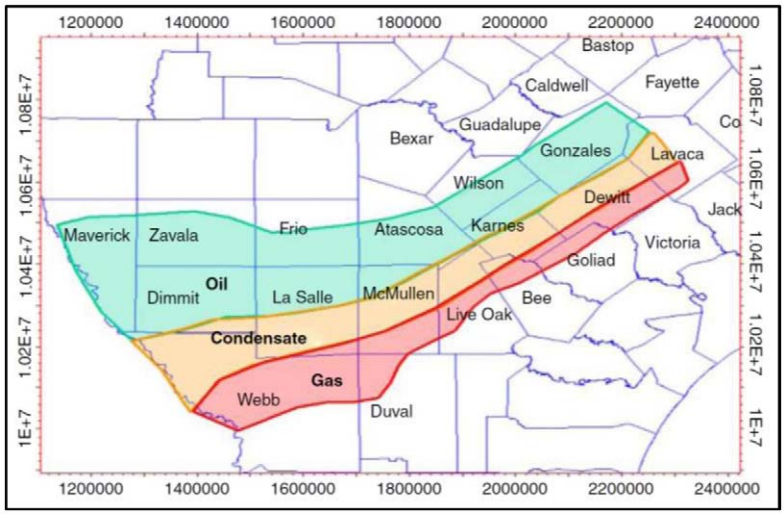

Figure 2—Maturation windows of the Eagle Ford shale (Ramirez and Aguilera, 2016).

To assist the discussion, let us recall the concept of hydrocarbon "containers". According to Hartmann and Beaumont (1999), a container is defined as "a reservoir system subdivision, consisting of a pore system, made up of one or more flow units, which respond as a unit when fluid is withdrawn". A flow unit is a "stratigraphically-continuous reservoir subdivision characterized by a similar pore type" (Hartmann and Beaumont, 1999). The distinctive geological aspect of an unconventional or upside- down fluid distribution in the Eagle Ford is explained using the concept of containers. Ramirez and Aguilera (2016) used rigorous numerical simulation to demonstrate that the vertical containment and fluids distribution in the Eagle Ford

shale has remained approximately the same over geological time (millions of years), with very small changes in the dry gas/condensate contact and the condensate/oil contact. The authors conclude that low natural fracturing and ultralow matrix permeability are the main factors controlling fluids migration.

The key as to why huff-and-puff gas injection works in shales relies on the concept of fluids containment, supported by the work of Ramirez and Aguilera (2016). This means that the injected gas flows into the hydraulic fractures and penetrates the tight matrix; and more importantly, does not generally escape or leak outside of the stimulated reservoir volume (SRV).

In the case of miscible gas injection, the recovery mechanisms leading to improved oil recovery include: 1) oil swelling, 2) oil viscosity and interfacial tension reduction, and 3) reservoir repressurization (Alharthy et al., 2017). Nevertheless, numerical simulation studies by Fragoso et al. (2018a) investigate the effect of immiscible huff-and-puff dry gas injection in shales (100% CH_4), without any mole percentage of heavier ends, and still show outstanding improvement in oil recoveries (Figure 3). Since the injected fluid in Fragoso et al.'s study does not reach miscibility with the reservoir oil, the main controlling factor by means of dry gas injection comes down to reservoir repressurization.

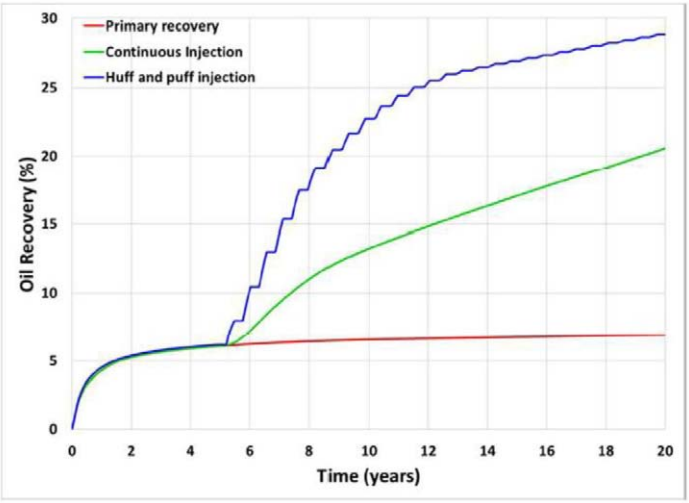

Figure 3—Oil recovery factor in the oil container of the Eagle Ford shale by huff-and-gas injection using dry gas (Fragoso et al., 2018a).

An additional mechanism may be the responsible for some of the increases in oil recovery. Given that at typical shales depth (8,000 ft, or more) the minimum principal stress is horizontal, it can be anticipated that hydraulic fractures are vertical (or of high inclination), and perpendicular to the direction of the minimum principal horizontal stress (Hubbert and Willis, 1957). In this scenario, gravity segregation with counterflow may play a role, with the injected gas moving up the hydraulic fractures and pushing oil down towards the horizontal well. In naturally fractured reservoirs, this mechanism can lead to high oil recovery factors. A good example is the Haft Kel reservoir (Aguilera, 2006), a prolific and thick naturally fractured reservoir in Iran characterized by significant vertical fracturing. Even in conventional reservoirs (without any fracturing), a primary drive mechanism by gravity segregation (or gravity drainage) can yield ultimate oil recovery factors as high as 80% (Ahmed, 2006). However, for stimulated shale reservoirs, the hypothesis on the occurrence of gravity segregation with counterflow requires further investigation in the laboratory. Thus far, the idea is only supported by some numerical simulation results showing that ultimate oil recoveries from shales by means of huff-and-puff gas injection can indeed be higher than those from conventional reservoirs performing under secondary recovery (Fragoso et al., 2018b).

Material Balance

The domain of the tank material balance presented in this paper corresponds to the oil container of a shale reservoir. Stress-sensitive porosity and permeability are not considered in this study. The portion of the material in this section dealing with primary recovery for undersaturated and saturated reservoirs was originally published by Aguilera (2006). The calculation of fractional oil recovery for saturated reservoirs that are above the bubble point at discovery, and most importantly, the treatment of huff-and- puff gas injection with the use of a new MBE, are the key contributions of this paper.

The MBE considers a dual porosity model made up of matrix and fractures. The porosity of the matrix system is represented by ϕ_{mt}, and comprises both the organic and the inorganic matrix. The porosity of the fractured system, ϕ_2, includes natural and hydraulic fractures.

Undersaturated Reservoirs

The MBE for an undersaturated oil reservoir is (Craft and Hawkins, 1959):

$$NB_{oi}C_{oe}\Delta p = N_p B_o + W_p B_w - W_e \tag{1}$$

Because, in general, shales do not have down-dip water leg, both the water production and water influx terms (W_pB_w and W_e, respectively) may be neglected in Equation (1). There are, however, some exceptions, for example, the Antrim shale in Michigan (Orozco, 2016). In such cases, the unsteady water influx from a naturally fractured aquifer and its effect on reservoir performance may be handled with published methodologies by Aguilera (1988) and Aguilera (2007). If the aquifer does not present significant level of fracturing, the classical method of Van Everdingen and Hurst (Craft and Hawkins, 1959) may be used.

Equation (1) allows calculating the fractional oil recovery for any pressure drop; or estimating the cumulative oil production N_p when the original oil in place N is known; or calculating N when production and pressure history are available.

The effective oil compressibility C_{oe} is determined by:

$$C_{oe} = \frac{C_o S_o + C_w S_w + C_r}{S_o} \tag{2}$$

For a fractured shale reservoir, the effective oil compressibility is modified to account for the compressibility of the fracture system:

$$C_{oe} = \frac{C_o S_{om}\phi_m + C_o S_{of}\phi_2 + C_w S_{wm}\phi_m + C_w S_{wf}\phi_2 + C_m\phi_m + C_f\phi_2}{S_{om}\phi_m + S_{of}\phi_2} \tag{3}$$

For practical purposes, the effective oil compressibility above the bubble point may be considered as a constant value.

Saturated Reservoirs

Aguilera (2006) introduced a material balance in finite difference form for estimating the recovery as a function of time in naturally fractured reservoirs performing below the bubble point. The MBE is:

$$\Delta\left(\frac{N_p}{N}\right)_{i+1} = \frac{\left[1-\left(\frac{N_p}{N_t}\right)_i\right]\Delta\left[\frac{B_o}{B_g} - R_s\right] - B_{ob}(1+m)\Delta\left(\frac{1}{B_g}\right)\left\langle 1+\left\{\left[(1-\omega)C' + \omega C''\right](\Delta p)\right\}\right\rangle}{\left(\frac{B_o}{B_g} - R_s\right)_{i+1} + R_{avg}(1-I_g)} \tag{4}$$

The symbol Δ in Equation (4) represents the change of the corresponding variable from pressure step i to pressure step $i+1$. Parameter ω represents the fraction of OOIP stored in the fractures. Equations for all PVT properties as a function of p must be known in advance.

The equation for the oil saturation is (Craft and Hawkins, 1959):

$$S_o = \left(1 - \frac{N_p}{N}\right)\frac{B_o}{B_{ob}}\left(1 - S_{wi}\right) \tag{5}$$

Effective matrix compressibility (C') and effective fracture compressibility (C'') are defined by:

$$C' = \frac{C_w S_{wm} + C_m}{1 - S_{wm}} \tag{6}$$

$$C'' = \frac{C_w S_{wf} + C_f}{1 - S_{wf}} \tag{7}$$

The instantaneous gas-oil ratio R (or GOR, in SCF/STB) is determined from (Craft and Hawkins, 1959):

$$R_{i+1} = 5.615\left(R_s + \frac{k_{rg}\mu_o B_o}{k_{ro}\mu_g B_g}\right)_{i+1} \tag{8}$$

The calculation approach for estimating recovery as a function of pressure and time is carried out throughout the following steps:

1. Perform a conventional material balance for only the matrix system, using the relative permeabilities of the matrix, and estimate the matrix oil saturation (S_{om}) as a function of pressure. Note that these calculations are only necessary when the evolution of oil and gas saturation within the fractures is required.
2. Determine the partitioning coefficient $v = \phi_2/\phi$, and calculate the average initial water saturation of the composite system of matrix and fractures from:

$$S_{wi} = S_{wim}\left(1 - v\right) + S_{wif} v \tag{9}$$

3. Assume a fractional oil recovery $(N_p/N)_{i+i}$ at a new reservoir pressure of interest. Next, calculate the oil saturation from Equation (5), and the gas saturation of the composite system from:

$$S_{g_{i+1}} = 1 - S_{o_{i+1}} - S_{wi} \tag{10}$$

4. Using the matrix oil saturation from Step 1, determine oil saturation in the fractures from Equation (11). Aguilera (2006) indicates that the calculation of S_{of} is highly sensitive to the values of S_{om}, and that poor S_{om} data will cause non-realistic values of S_{of}, and consequently of S_{gf}

$$S_{of_{i+1}} = \frac{S_{o_{i+1}} - S_{om_{i+1}}\left(1 - v\right)}{v} \tag{11}$$

5. Compute the instantaneous gas-oil ratio from Equation (8). If no laboratory data is available for the relative permeabilities, calculate them from the following equations that assume 45-degree straight lines for the fracture system:

$$S_{i+1} = \frac{S_{g_{i+1}} - S_{gc}}{1 - S_{gc} - S_{or} - S_{wi}} \tag{12}$$

$$k_{rg_{i+1}} = k^o_{rg} S_{i+1} \tag{13}$$

$$k_{roi+1} = k_{ro}^{o}\left(1 - S_{i+1}\right) \tag{14}$$

6. Use Equation (4) to calculate the incremental fractional oil recovery $\Delta(N_p/N)_{i+1}$. Then, calculate the cumulative fractional oil recovery at pressure $i+1$ from:

$$\left(\frac{N_p}{N}\right)_{i+1} = \Delta\left(\frac{N_p}{N}\right)_{i+1} + \left(\frac{N_p}{N}\right)_{i} \tag{15}$$

7. Compare the computed cumulative fractional oil recovery from Step 6 with that one assumed in Step 3. When they are equal, or when a predetermined tolerance is achieved, move to the next pressure step and repeat Steps 3 to 7.

   Up to this point, the procedure allows calculation of oil recovery as a function of pressure. The following steps permit computation of oil recovery as a function of time. For this purpose, an equation for oil production rate and the corresponding decline must be introduced. In practice, shale oil wells exhibit hyperbolic declines, but "stepwise" exponential declines between two values of average reservoir pressure can represent fairly the production performance. This approach is implemented in this paper.

8. Calculate the productivity index J_{i+1} from:

$$J_{i+1} = J_1 \frac{k_{ro_{i+1}}\left(\mu_o B_o\right)_1}{k_{ro_1}\left(\mu_o B_o\right)_{i+1}} \tag{16}$$

9. Determine the oil production rate (STB/D) from:

$$q_{oi+1} = J_{i+1}\left(p_{i+1} - p_{wf\,i+1}\right) W_{i+1}, \tag{17}$$

   where W_{i+1} is the number of producing wells at pressure $i+1$ with the same productivity index.

10. Determine the cumulative oil production N_{pi+1}, and the incremental cumulative oil production ΔN_{pi+i}, using:

$$N_{p_{i+1}} = \left(\frac{N_p}{N}\right)_{i+1} N \tag{18}$$

$$\Delta N_{p_{i+1}} = N_{p_{i+1}} - N_{p_i} \tag{19}$$

11. Compute the yearly exponential production decline when the oil rate changes from q_{oi} to q_{oi+1}, from:

$$a_{i+1} = 365\left(\frac{q_{o_i} - q_{o_{i+1}}}{\Delta N_{p_{i+1}}}\right) \tag{20}$$

12. Calculate the incremental time in years associated with the change of oil rate from q_{oi} to q_{oi+1}:

$$\Delta t_{i+1} = \frac{\ln\left(\frac{q_{o_i}}{q_{o_{i+1}}}\right)}{a_{i+1}} \tag{21}$$

   Also, compute the cumulative time from:

$$t_{i+1} = t_i + \Delta t_{i+1} \tag{22}$$

13. Determine the gas production rate in MMSCF/D from:

$$q_{g_{i+1}} = \left(\frac{q_{oi+1} R_{i+1}}{10^6} \right) \tag{23}$$

14. Calculate the incremental cumulative gas production ΔG_{pi+1}, and the cumulative gas production G_{pi+i}, using:

$$\Delta G_{p_{i+1}} = 365 \left(q_g \Delta t \right)_{i+1} \tag{24}$$

$$G_{p_{i+1}} = G_{p_i} + \Delta G_{p_{i+1}} \tag{25}$$

15. Repeat Steps 3 to 14 for a new reservoir pressure. Continue the same procedure until reaching the abandonment pressure.

Notice that Steps 8 to 14 also hold for the case of undersaturated reservoirs to calculate recovery as a function of time, but the following modifications must be introduced:

- The gas-oil ratio is simply equal to the solution gas-oil ratio R_{sb}.
- Do not use Equation (16) for computing the productivity index. Use, instead:

$$J_{i+1} = \frac{\left(k_{hf} w_{hf} + k_2 h \right)}{141.2 \left(\mu_o B_o \right)_{i+1} \ln \left(\frac{r_{eh}}{r_w^{'}} - 0.5 + S \right)}, \tag{26}$$

where r_{eh} is the drainage radius of the horizontal well assuming an elliptical drainage area (Joshi, 1991):

$$r_{eh} = \sqrt{\left(\frac{L}{2} + r_{ev} \right) r_{ev}}\ , \tag{27}$$

and r_w' is the modified wellbore radius for a hydraulically fractured well:

$$r_w^{'} = \frac{x_{hf}}{2} \tag{28}$$

Initially Undersaturated Reservoir that reaches Saturation Conditions

For the case when the reservoir is initially undersaturated but eventually reaches saturation conditions due to depletion, a combination of both MBEs discussed above should be implemented. The cumulative oil recovery must be calculated as follows:

1. If the average reservoir pressure is equal to or above the bubble point, then the true cumulative fractional oil recovery is estimated from Equation (1). Hence, the cumulative oil production N_p is given by the product of (N_p/N) times the original oil-in-place N.
2. If the average reservoir pressure is less than the bubble point, the true cumulative fractional oil recovery is calculated from:

$$\left(\frac{N_p}{N} \right)_{T_{i+1}} = \left\{ \left[1 - \left(\frac{N_p}{N} \right)_b \right] \left(\frac{N_p}{N} \right)_{i+1} \right\} + \left(\frac{N_p}{N} \right)_b, \tag{29}$$

where $(N_p/N)_b$ is the cumulative fractional oil recovery at the bubble point, and $(N_p/N)_{i+1}$ is computed from Equation (15). Thus, the cumulative oil production will be the product of the result from Equation (29) times the original oil-in-place N.

Treatment of Huff-and-Puff Gas Injection

This section deals with material balance calculations of huff-and-puff methane gas injection using the same well as producer and injector. Notice that the MBE presented in Equation (4) includes a continuous gas injection index I_g. This index corresponds to the fraction of produced gas that is reinjected in the reservoir through a separate injection well. However, as explained in the Introduction, this paper only focuses on huff-and-puff gas injection.

The following observations and assumptions need to be clearly stated:

1. The reservoir produces fluids under primary recovery during a certain period of time (e.g., 2 – 5 years), as shown in Figure 1.
2. The injected gas has a composition of 100% methane (CH_4) and does not reach miscibility with the reservoir oil.
3. The injected gas is contained within the target SRV, i.e., it flows into the hydraulic fractures and penetrates the tight matrix, and more importantly, does not escape or leak outside of the SRV. This statement stems from the 1 million-year simulation performed by Ramirez and Aguilera (2016). They demonstrated that the fluids did not move during this time out of their respective containers.
4. Part of the gas volume injected during the huff period is produced during the puff period.
5. Gas injection may start when the average reservoir pressure is either above or slightly below the bubble point. In the second case, the first gas injection cycle is able to restore the average reservoir pressure above the bubble point. Therefore, any amount of free gas goes back in solution, and the injected gas remains free, creating a sort of secondary gas cap that grows as injection goes on. Since the SRV is fixed, the gas saturation of the composite system of matrix and fractures increases progressively.
6. As long as the huff-and-puff gas injection continues, the average reservoir pressure does not fall below the bubble point; hence, the reservoir oil remains undersaturated.
7. For the injection (or huff) period, the problem consists of determining the unknown average reservoir pressure following injection.
8. For the production (or puff) period, the problem consists of determining the fractional oil recovery, and oil and gas cumulative production and rates as a function of time.

Assumptions 5 and 6 are supported by detailed numerical simulation studies performed by Fragoso et al. (2018a) (Figure 4). The authors use models with reservoir and fluid properties of the Eagle Ford shale very similar to those used in the case study discussed later in this paper. Thus, under the stated assumptions and observations, there are two different material balance equations to be solved for each injection/production huff-and-puff cycle.

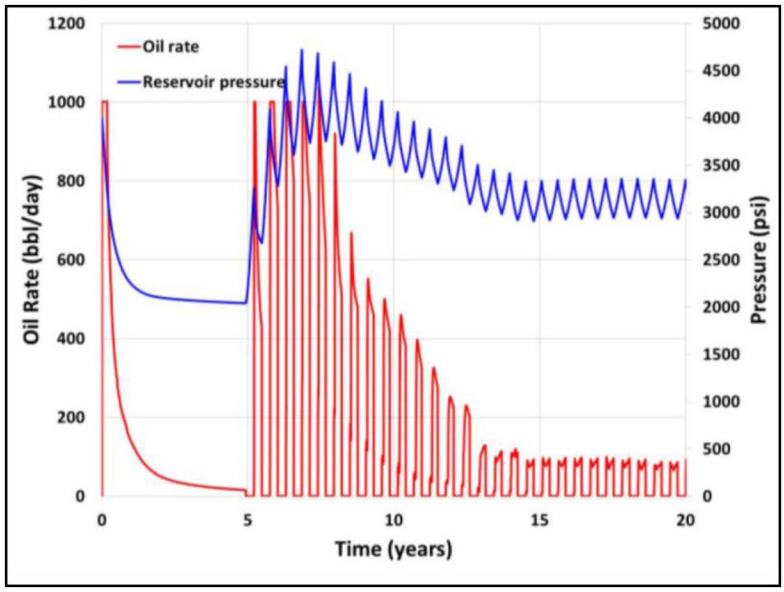

Figure 4—Oil production rate and average reservoir pressure in the oil container of the Eagle Ford for the huff-and-puff gas injection case (Fragoso et al., 2018a).

Calculating the Average Reservoir Pressure Following Injection

For the injection (or huff) period, the MBE assumes an undersaturated reservoir, i.e., Equation (1), with the inclusion of a term that accounts for both the cumulative gas injection and production associated to the injected gas. Thus, the modified MBE (ignoring water production and water influx) is:

$$N_r B_{oI} C_{oe}(p_I - p) = N_p B_o - \left(G^{inj} - G_p^{inj}\right) B_g^{inj} \tag{30}$$

where N_r and p_I are the remaining oil-in-place and the average reservoir pressure before the start of each injection cycle, respectively; p is the unknown average reservoir pressure following injection; B_{oI} is the oil formation volume factor at p_i; G^{inj} is the cumulative gas injection in STB; G_p^{inj} is the cumulative gas production associated to the injected gas (also in STB); and B_g^{inj} is the formation volume factor of the injected gas.

Because the behavior of the formation volume factor of both the reservoir oil and the injected gas are known in advance, then Equation (30) can be written as:

$$N_r B_{oI} C_{oe}(p_I - p) = N_p f(p) - \left[\left(G^{inj} - G_p^{inj}\right) g(p)\right], \tag{31}$$

where $f(p) = B_o$ is a linear function, and $g(p) = B_g^{inj}$ is a power function. Equation (31) is a non-linear equation for p. The non-linearity is caused by the strong and highly non-linear pressure-dependence of the formation volume factor of the injected gas (or of any real gas, for that matter). Equation (31) is rearranged as:

$$p - p_I + \left(\frac{N_p}{N_r B_{oI} C_{oe}}\right) f(p) - \left[\frac{\left(G^{inj} - G_p^{inj}\right)}{N_r B_{oI} C_{oe}}\right] g(p) = 0 \tag{32}$$

We define the function $F(p)$:

$$F(p) = p - p_I + \left(\frac{N_p}{N_r B_{oI} C_{oe}}\right) f(p) - \left[\frac{\left(G^{inj} - G_p^{inj}\right)}{N_r B_{oI} C_{oe}}\right] g(p) \tag{33}$$

Thus, for each cycle, the problem of determining the average reservoir pressure following injection is reduced to solving the non-linear equation:

$$F(p)=0 \tag{34}$$

Given its quick-convergence feature, the iterative Newton-Raphson method is deployed (Chapra and Canale, 2009) for the calculation. Equation (34), written in the Newton-Raphson numerical form, is:

$$p^{k+1}=p^{k}-\frac{F(p^{k})}{F'(p^{k})}, \tag{35}$$

where $F'(p^k)$ is the first derivative of function $F(p)$ evaluated at the p value calculated in the k-th iteration. A good initial guess p^0 for the unknown pressure may be simply p_I. Notice that, as far as the calculation of p is concerned, N_p, N_r, B_{oI}, C_{oe}, G^{inj} and G_p^{inj} are all constants. Therefore, the first derivative $F'(p)$ can be readily calculated. Newton-Raphson iterations are performed until reaching a predetermined tolerance level, for example, 10^{-6}.

Calculating Fractional Oil Recovery for the Puff Period

For the production (or puff) period, the fractional oil recovery is calculated from Equation (1) without any modifications. This is so because the increased average reservoir pressure accounts implicitly for the effect of the gas injection. However, an important observation is that the computed fractional recovery and the corresponding cumulative oil production are associated with the remaining oil-in-place N_r, not the initial oil-in-place N.

Generalized Calculation Approach

The generalized procedure for material balance calculations including the effect of huff-and-puff gas injection is as follows:

1. Run the material balance calculations for the primary recovery stage as per the methodologies explained for undersaturated and saturated reservoirs, or the combination of both, based on the case under consideration.

   From this point, the procedure applies for each injection/production huff-and-puff cycle. Note that pressure step i represents the beginning of the injection period; pressure step $i+1$ corresponds to the end of the injection period, i.e., the beginning of the production period; and pressure step $i+2$ corresponds to the end of the production period. Thus, the oil production rate is set equal to zero between pressure steps i and $i+1$.
2. Calculate the remaining oil-in-place at the beginning of the gas injection cycle, from:

$$N_{r_{i+1}}=N-N_{p_i} \tag{36}$$

3. Determine the injected gas volume at standard conditions, in STB, using:

$$\Delta G_{i+1}^{inj}=\frac{10^{6}\,q_{g_{i+1}}^{inj}\,\Delta t_{i+1}^{inj}}{5.615}, \tag{37}$$

   where q_{gi+1}^{inj} is the gas injection rate in MMSCF/D, and Δt_{i+1}^{inj} is the duration of the injection period, in days. For production forecasting purposes, both of these parameters are known and given by the injection schedule. For history matching purposes, only the duration of the injection period is known. Should this be the case, assume a value for the gas injection rate (0.1 to 5 MMSCF/D is a recommended range) and proceed with the calculations.
4. Determine the cumulative gas injection:

$$G_{i+1}^{inj} = G_i^{inj} + \Delta G_{i+1}^{inj} \tag{38}$$

5. Use the Newton-Raphson iterative equation to calculate the new average reservoir pressure p_{i+1} following gas injection:

$$p_{i+1}^{k+1} = p_{i+1}^{k} - \left\{ \frac{p_{i+1}^{k} - p_I + \left(\frac{N_{p_i}}{N_{r_{i+1}} B_{oI} C_{oe}} \right) f(p_{i+1}^{k}) - \left[\frac{\left(G_{i+1}^{inj} - G_{p_i}^{inj} \right)}{N_{r_{i+1}} B_{oI} C_{oe}} \right] g(p_{i+1}^{k})}{1 + \left(\frac{N_{p_i}}{N_{r_{i+1}} B_{oI} C_{oe}} \right) f'(p_{i+1}^{k}) - \left[\frac{\left(G_{i+1}^{inj} - G_{p_i}^{inj} \right)}{N_{r_{i+1}} B_{oI} C_{oe}} \right] g'(p_{i+1}^{k})} \right\} \tag{39}$$

Note that the difference G_{i+1}^{inj} - G_{pi}^{inj} corresponds to the volume occupied by the injected gas within the reservoir (measured at standard conditions) at the end of the injection period. Moreover, for the first injection/production huff-and-puff cycle, G_{pi}^{inj} is equal to zero.

6. Calculate productivity index J_{i+1}:

$$J_{i+1} = \frac{\left(k_{hf} w_{hf} + k_2 h \right)}{141.2 \left(\mu_o B_o \right)_{i+1} \ln \left(\frac{r_{eh}}{r_w'} - 0.5 + S \right)} \tag{40}$$

7. Calculate the oil production rate q_{oi+1} when the well is opened to production:

$$q_{oi+1} = J_{i+1} \left(p_{i+1} - p_{wf\,i+1} \right) W_{i+1} \tag{41}$$

8. For history matching purposes, compare the value of q_{oi+1} with the actual oil production rate when the well is opened to production. If they are different, assume a new gas injection rate q_{gi+1}^{inj} and repeat Steps 3 to 8 until the calculated q_{oi+1} is equal to the actual oil rate, or until certain tolerance is reached. For production forecasting purposes, skip Step 8 and move on to Step 9.

9. Assume a value of average reservoir pressure p_{i+2} lower than the computed p_{i+1}, and calculate the incremental fractional oil recovery associated to the pressure drop p_{i+1} - p_{i+2}, using:

$$\Delta \left(\frac{N_p}{N_r} \right)_{i+2} = \frac{B_{o_{i+1}} C_{oe} \left(p_{i+1} - p_{i+2} \right)}{B_{o_{i+2}}} \tag{42}$$

10. Compute the incremental cumulative oil recovery:

$$\Delta N_{p_{i+2}} = \Delta \left(\frac{N_p}{N_r} \right)_{i+2} N_{r_{i+1}} \tag{43}$$

11. Determine the productivity index J_{i+2}:

$$J_{i+2} = \frac{\left(k_{hf} w_{hf} + k_2 h \right)}{141.2 \left(\mu_o B_o \right)_{i+2} \ln \left(\frac{r_{eh}}{r_w'} - 0.5 + S \right)} \tag{44}$$

12. Calculate the oil production rate q_{oi+2}:

$$q_{oi+2} = J_{i+2} \left(p_{i+2} - p_{wf\,i+2} \right) W_{i+1} \tag{45}$$

13. Compute the yearly exponential production decline when the oil rate changes from q_{oi+1} to q_{oi+2}, from:

$$a_{i+2} = 365\left(\frac{q_{o_{i+1}} - q_{o_{i+2}}}{\Delta N_{p_{i+2}}}\right) \tag{46}$$

14. Calculate the incremental time in years that it takes for the oil production rate to change from q_{oi+1} to q_{oi+2}:

$$\Delta t_{i+2} = \frac{\ln\left(\frac{q_{o_{i+1}}}{q_{o_{i+2}}}\right)}{a_{i+2}} \tag{47}$$

15. Compare the calculated incremental time with the actual duration of the puff period, which is given either by the injection schedule (for forecasting purposes), or by the production record (for history matching purposes). Repeat Steps 9 to 15 until the calculated Δt_{i+2} is equal to the actual production time of the huff-and-puff cycle, or until certain tolerance level is fulfilled.
16. Determine the cumulative oil production from:

$$N_{p_{i+2}} = \Delta N_{p_{i+2}} + N_{p_{i+1}} \tag{48}$$

Note that, for each individual cycle, $N_{pi+1} = N_{pi}$, because there is no production during the injection period comprised between pressure steps i and $i+1$.

17. Estimate the total true cumulative fractional oil recovery:

$$\left(\frac{N_p}{N}\right)_{i+2} = \frac{N_{p_{i+2}}}{N}$$

18. Compute the cumulative time from:

$$t_{i+1} = t_i + \Delta t_{i+1}^{inj} \tag{49}$$

$$t_{i+2} = t_{i+1} + \Delta t_{i+2} \tag{50}$$

19. Calculate the total gas saturation of the composite system at p_{i+1} and p_{+2}, from:

$$S_{g_{i+1}} = \frac{\left(G_{i+1}^{inj} - G_{p_i}^{inj}\right)B_{g_{i+1}}^{inj}}{PV} \tag{51}$$

$$S_{g_{i+2}} = \frac{\left(G_{i+1}^{inj} - G_{p_i}^{inj}\right)B_{g_{i+2}}^{inj}}{PV}, \tag{52}$$

where PV is the reservoir pore volume (fixed), given by:

$$PV = 7{,}758Ah\phi, \tag{53}$$

and ϕ is the total porosity of the shale $(\phi_{mt} + \phi_2)$. The oil saturation of the composite system may also be determined, by:

$$S_{o_{i+1}} = 1 - S_{g_{i+1}} - S_{wi} \tag{54}$$

$$S_{o_{i+2}} = 1 - S_{g_{i+2}} - S_{wi} \tag{55}$$

20. Determine oil and gas relative permeabilities at pressures p_{i+1} and p_{i+2} using Equations (12), (13) and (14) and the gas saturations from Step 19.
21. Compute the instantaneous GOR at pressures p_{i+1} and p_{i+2}, from:

$$R_{i+1} = 5.615\left[R_{sb} + \left(\frac{k_{rg}\mu_o B_o}{k_{ro}\mu_g^{inj} B_g^{inj}}\right)_{i+1}\right] \quad (56)$$

$$R_{i+2} = 5.615\left[R_{sb} + \left(\frac{k_{rg}\mu_o B_o}{k_{ro}\mu_g^{inj} B_g^{inj}}\right)_{i+2}\right], \quad (57)$$

where μ_g^{inj} is the viscosity of the injected gas.

22. Determine the gas production rate in MMSCF/D from:

$$q_{g_{i+2}} = \left(\frac{q_{o_{i+2}} R_{i+2}}{10^6}\right) \quad (58)$$

23. Calculate the incremental cumulative gas production associated to injection, ΔG_{pi+2}^{inj}, and the cumulative gas production due to injection G_{pi+2}^{inj}, using:

$$\Delta G_{p_{i+2}}^{inj} = 365\left(q_g \Delta t\right)_{i+2} \quad (59)$$

$$G_{p_{i+2}}^{inj} = \Delta G_{p_{i+2}}^{inj} + G_{p_{i+1}}^{inj} \quad (60)$$

24. Determine the total cumulative gas production:

$$G_{p_{i+2}} = G_{p_{i+2}}^{inj} + G_{p_{i+1}} \quad (61)$$

25. Repeat Steps 3 to 24 for as many huff-and-puff cycles as needed, until completing the entire injection schedule (production forecasting), or until fitting the available production history (history matching).

Case Study of the Eagle Ford Shale

The applicability of the proposed material balance is tested with real data from a producing horizontal well in the Eagle Ford shale undergoing huff-and-puff gas injection.

The Eagle Ford shale is the most prolific unconventional play in the United States. Located in south Texas, it extends over an area of approximately 45,000 km^2, and its significant importance relies on its capability of producing both natural gas and more oil than any other shale play in the US (Railroad Commission of Texas, 2017). With an average thickness of 250 feet, the Eagle Ford rests between the Austin Chalk and the Buda Limestone, with depths ranging between 4,000 and 12,000 ft. Oil production from this play reported by the Railroad Commission of Texas (Figure 5) illustrates its importance for the US energy sector.

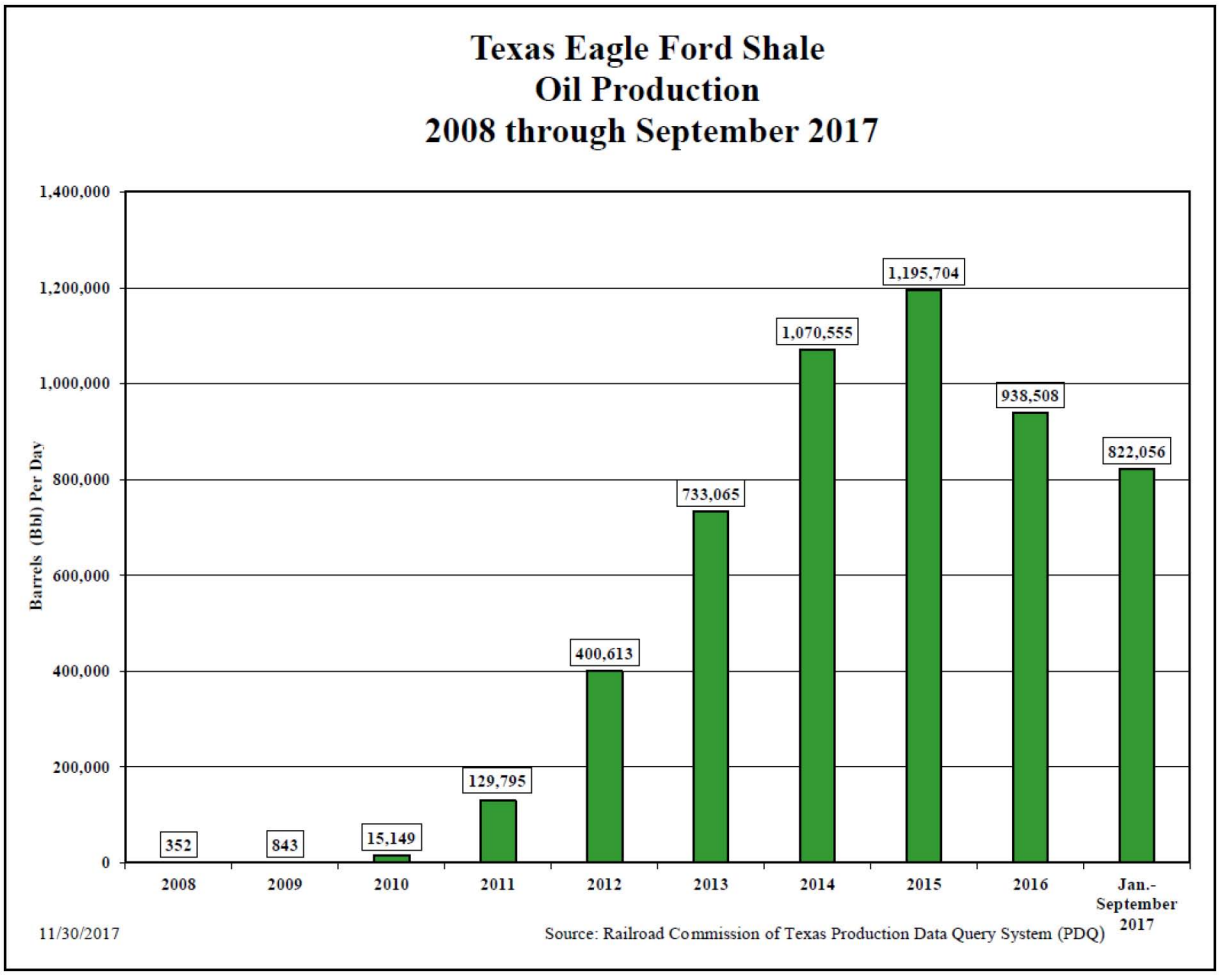

Figure 5—Eagle Ford daily oil production since 2010 (Railroad Commission of Texas, 2017).

The proposed material balance is used for matching the oil production history of well Eagle Ford 1 (including its 5 huff-and-puff cycles), and then for estimating the huff-and-puff production forecast of the same well over 120 months (10 years). The name of the well is fictitious, but the production data are real. Oil production history for well Eagle Ford 1 is plotted in Figure 6, and the corresponding digits are presented in Table 1. Reservoir and wellbore parameters for the material balance calculations are summarized in Table 2, and are similar to those used by Fragoso et al. (2018b) in a numerical simulation study. PVT properties of the reservoir fluid are shown in Table 3. Table 4 shows the gas injection rates used for fitting the oil rate during the 5 huff-and-puff cycles.

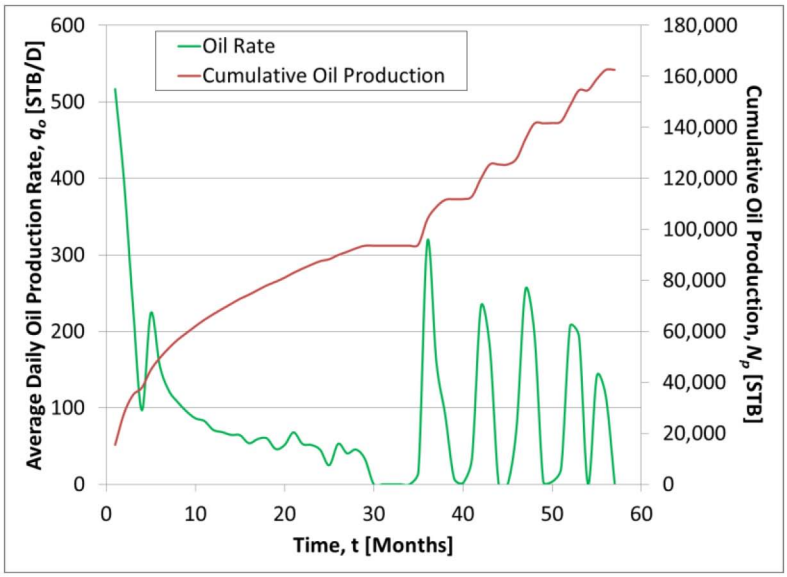

Figure 6—Oil production history for well Eagle Ford 1.

Table 1—Oil production history for well Eagle Ford 1.

Time [Months]	Average Oil Production Rate [STB/D]	Cumulative Oil Production [STB]	Time [Months]	Average Oil Production Rate [STB/D]	Cumulative Oil Production [STB]
1	516.87	15,506	30	0.00	93,608
2	396.32	27,792	31	0.00	93,608
3	233.45	35,029	32	0.00	93,608
4	96.83	37,934	33	0.07	93,610
5	223.97	44,877	34	0.03	93,611
6	155.47	49,541	35	16.27	94,099
7	123.06	53,356	36	317.42	103,939
8	107.74	56,696	37	161.40	108,781
9	95.43	59,368	38	90.90	111,599
10	86.35	62,045	39	7.90	111,844
11	82.87	64,531	40	1.70	111,895
12	71.23	66,739	41	33.58	112,936
13	68.30	68,788	42	231.93	119,894
14	64.58	70,790	43	179.90	125,471
15	64.26	72,782	44	0.00	125,471
16	53.83	74,397	45	0.00	125,471
17	59.32	76,236	46	74.35	127,776
18	60.20	78,042	47	254.53	135,412
19	46.29	79,477	48	197.23	141,526
20	51.45	81,072	49	3.10	141,619
21	67.93	82,974	50	3.48	141,727
22	52.90	84,614	51	20.84	142,373
23	51.53	86,160	52	206.67	148,573

Time [Months]	Average Oil Production Rate [STB/D]	Cumulative Oil Production [STB]	Time [Months]	Average Oil Production Rate [STB/D]	Cumulative Oil Production [STB]
24	45.06	87,557	53	193.48	154,571
25	25.07	88,309	54	0.17	154,576
26	53.00	89,952	55	141.55	158,964
27	40.61	91,211	56	115.74	162,552
28	45.60	92,579	57	1.39	162,591
29	33.19	93,608			

Huff-and-Puff Schedule		
Huff-and-Puff Cycle	**Duration of Injection Period [Months]**	**Duration of Production Period [Months]**
1	5.80	3.58
2	2.50	2.11
3	2.50	2.61
4	2.88	2.22
5	0.90	2.12

Table 2—Reservoir and wellbore parameters for material balance calculations of the case study.

Parameter	Symbol	Value	Units
Initial reservoir pressure	p_i	6,000	psi
Bubble point pressure	p_b	2,400	psi
Original oil-in-place	N	1.298	MMSTB
Matrix original-oil-in-place	N_m	1.277	MMSTB
Fractures original-oil-in-place	N_f	0.021	MMSTB
Matrix water saturation	S_{wm}	0.50	Fraction
Matrix oil saturation	S_{om}	0.50	Fraction
Fractures water saturation	S_{wf}	0.10	Fraction
Fractures oil saturation	S_{of}	0.90	Fraction
Water compressibility	C_w	3.00E-06	psi^{-1}
Oil compressibility	C_o	1.00E-05	psi^{-1}
Matrix compressibility	C_m	1.00E-06	psi^{-1}
Residual oil saturation	S_{or}	0.20	Fraction
Critical gas saturation	S_{gc}	0.00	Fraction
Oil relative permeability at critical gas saturation	k_{ro}^0	1.00	–
Gas relative permeability at residual oil saturation	k_{rg}^0	1.00	–
Inorganic matrix porosity	ϕm	0.05000	Fraction
Organic matrix porosity	ϕ_{org}	0.00970	Fraction
Matrix porosity	ϕ_{mt}	0.05970	Fraction
Fractures porosity (natural and hydraulic)	ϕ_2	0.00055	Fraction

Parameter	Symbol	Value	Units
Total shale porosity	ϕ	0.06025	Fraction
Partitioning coefficient	v	0.00913	Fraction
Reservoir temperature	T	686.67	R
Reservoir thickness	h	97.50	ft
Well drainage area	A	73.18	Acres
Hydraulic fracture half-length	x_{hf}	150	ft
Length of the horizontal well	L	3,750	ft
Skin factor	S	0	–
Permeability of natural fractures	k_2	0.3077	md
Flow capacity of hydraulic fractures	$k_{hf}w_{hf}$	10	md-ft
Total flow capacity of fractures	$k_{hf}w_{hf} + k_2h$	40	md-ft
Bottomhole flowing pressure	p_{wf}	2,000	psi
Abandonment pressure (for primary recovery stage)	p_{ab}	2,010	psi
Continuous gas injection index	I_g	0.00	–
Size of the gas cap	m	0.00	–
Specific gravity of the injected gas (100% CH_4)	SG	0.554	

Table 3—PVT data.

Pressure	Oil Formation Volume Factor	Gas-Oil Solution Ratio	Gas Formation Volume Factor	Oil Viscosity	Gas Viscosity
P	B_o	R_s	B_g	μ_o	μ_g
psi	RB/STB	SCF/STB	Vol/Vol	cp	cp
6,015	1.3866	671.38		0.8032	
5,515	1.3931	671.38		0.7678	
5,015	1.3999	671.38		0.7411	
4,515	1.4071	671.38		0.7109	
4,015	1.4149	671.38		0.6851	
3,515	1.4233	671.38		0.6630	
3,015	1.4328	671.38		0.6330	
2,400	1.4459	671.38		0.5978	
2,115	1.4063	596.53	0.00800	0.5968	0.01748
1,815	1.3723	521.17	0.00930	0.5982	0.01666
1,515	1.3372	448.88	0.01120	0.6110	0.01591
1,215	1.3038	376.74	0.01410	0.6438	0.01521
1,015	1.2823	330.85	0.01710	0.6779	0.01478
815	1.262	286.94	0.02150	0.7286	0.01437
615	1.2383	240.08	0.02860	0.7702	0.01391
415	1.2122	191.00	0.04250	0.8489	0.01340

Pressure	Oil Formation Volume Factor	Gas-Oil Solution Ratio	Gas Formation Volume Factor	Oil Viscosity	Gas Viscosity
P	B_o	R_s	B_g	μ_o	μ_g
psi	RB/STB	SCF/STB	Vol/Vol	cp	cp
215	1.1769	132.63	0.08080	0.9262	0.01260
15	1.0815	0.00	1.28230	1.1750	0.01094

Table 4—History-matching gas injection rates.

Huff-and-Puff Cycle	Gas Injection Rate, q_{ginj} [MMSCF/D]
1	1.50
2	0.50
3	0.80
4	0.50
5	0.50

Effective oil compressibility, computed from Equation (3), is equal to 1.49E-05. Equations (6) and (7) are used to determine compressibilities C' and C'' equal to 5.00E-06 and 1.44E-06, respectively. The irreducible water saturation of the composite system is determined to be 0.496, from Equation (9).

Results for the material balance calculations (including both history matching and production forecasting) are summarized in Table 5 and Table 6. For the primary recovery stage, 10-psi pressure steps were used in order to obtain smooth curves. However, for the sake of brevity, results are shown every 100 psi. As for gas injection calculations, notice the fast convergence of the Newton-Raphson method. This is reflected in Table 6 by the small number of iterations for calculating the average reservoir pressure following injection with a tolerance of 10^{-12} or lower.

Table 5—Material balance results.

P	S_o	S_g	GOR	N_p/N	N_p	J	q_o	t	q_g	G_p	t
psi	Fraction	Fraction	SCF/STB	%>	MMSTBO	STB/D/PSI	STB/D	Years	MMSCF/D	MMSCF	months
6,000	0.504	0.000	671.40	0.000%	0.00000	0.098	391.3	0	0.263	0.000	0.00
5,900	0.504	0.000	671.40	0.149%	0.00194	0.098	383.8	0.01	0.258	1.299	0.16
5,800	0.504	0.000	671.40	0.298%	0.00387	0.099	376.1	0.03	0.253	2.595	0.33
5,700	0.504	0.000	671.40	0.447%	0.00580	0.100	368.4	0.04	0.247	3.888	0.50
5,600	0.504	0.000	671.40	0.595%	0.00772	0.100	360.6	0.06	0.242	5.178	0.68
5,500	0.504	0.000	671.40	0.743%	0.00964	0.101	352.7	0.07	0.237	6.465	0.85
5,400	0.504	0.000	671.40	0.890%	0.01155	0.101	344.7	0.09	0.231	7.748	1.03
5,300	0.504	0.000	671.40	1.037%	0.01346	0.102	336.6	0.10	0.226	9.029	1.22
5,200	0.504	0.000	671.40	1.184%	0.01537	0.103	328.4	0.12	0.221	10.307	1.41
5,100	0.504	0.000	671.40	1.331%	0.01727	0.103	320.2	0.13	0.215	11.581	1.60
5,000	0.504	0.000	671.40	1.477%	0.01917	0.104	311.8	0.15	0.209	12.853	1.80
4,900	0.504	0.000	671.40	1.623%	0.02106	0.105	303.3	0.17	0.204	14.122	2.00

P	S_o	S_g	GOR	N_p/N	N_p	J	q_o	t	q_g	G_p	t
psi	Fraction	Fraction	SCF/STB	%>	MMSTBO	STB/ D/PSI	STB/D	Years	MMSCF/ D	MMSCF	months
4,800	0.504	0.000	671.40	1.768%	0.02295	0.105	294.7	0.18	0.198	15.387	2.21
4,700	0.504	0.000	671.40	1.913%	0.02483	0.106	286.1	0.20	0.192	16.650	2.42
4,600	0.504	0.000	671.40	2.058%	0.02671	0.107	277.3	0.22	0.186	17.910	2.64
4,500	0.504	0.000	671.40	2.203%	0.02858	0.107	268.4	0.24	0.180	19.166	2.86
4,400	0.504	0.000	671.40	2.347%	0.03045	0.108	259.3	0.26	0.174	20.420	3.10
4,300	0.504	0.000	671.40	2.491%	0.03232	0.109	250.2	0.28	0.168	21.671	3.34
4,200	0.504	0.000	671.40	2.634%	0.03418	0.110	241.0	0.30	0.162	22.919	3.59
4,100	0.504	0.000	671.40	2.777%	0.03604	0.110	231.6	0.32	0.155	24.163	3.85
4,000	0.504	0.000	671.40	2.920%	0.03789	0.111	222.1	0.34	0.149	25.405	4.11
3,900	0.504	0.000	671.40	3.063%	0.03974	0.112	212.5	0.37	0.143	26.644	4.39
3,800	0.504	0.000	671.40	3.205%	0.04159	0.113	202.7	0.39	0.136	27.880	4.69
3,700	0.504	0.000	671.40	3.347%	0.04343	0.113	192.8	0.42	0.129	29.113	4.99
3,600	0.504	0.000	671.40	3.488%	0.04527	0.114	182.8	0.44	0.123	30.342	5.31
3,500	0.504	0.000	671.40	3.629%	0.04710	0.115	172.6	0.47	0.116	31.569	5.65
3,400	0.504	0.000	671.40	3.770%	0.04893	0.116	162.3	0.50	0.109	32.793	6.01
3,300	0.504	0.000	671.40	3.911%	0.05075	0.117	151.8	0.53	0.102	34.013	6.39
3,200	0.504	0.000	671.40	4.051%	0.05257	0.118	141.2	0.57	0.095	35.231	6.80
3,100	0.504	0.000	671.40	4.191%	0.05439	0.119	130.4	0.60	0.088	36.445	7.24
3,000	0.504	0.000	671.40	4.331%	0.05620	0.119	119.4	0.64	0.080	37.656	7.72
2,900	0.504	0.000	671.40	4.470%	0.05801	0.120	108.3	0.69	0.073	38.864	8.24
2,700	0.504	0.000	671.40	4.748%	0.06161	0.122	85.6	0.79	0.057	41.269	9.47
2,500	0.504	0.000	671.40	5.024%	0.06520	0.124	62.1	0.92	0.042	43.658	11.08
2,400	0.504	0.000	671.40	5.162%	0.06698	0.125	50.1	1.01	0.034	44.845	12.13
2,300	0.495	0.009	1,808.55	6.050%	0.0785	0.120	35.9	1.75	0.065	59.321	20.98
2,200	0.487	0.017	2,724.16	6.647%	0.08625	0.117	23.4	2.47	0.064	76.783	29.63
Huff-and-puff gas injection starts. Total number of huff-and-puff cycles is 14 including 5 cycles with available production history)											
4,924	0.446	0.057	3,198.17	6.647%	0.08625	0.104	305.4	2.95	0.977	76.783	35.43
3,500	0.424	0.079	3,542.59	8.601%	0.11161	0.115	172.6	3.25	0.299	143.414	39.01
4,543	0.449	0.055	2,914.68	8.601%	0.11161	0.107	272.2	3.46	0.793	143.414	41.51
3,700	0.437	0.067	3,075.53	9.740%	0.12640	0.113	192.8	3.64	0.593	181.510	43.62
4,572	0.444	0.060	3,173.55	9.740%	0.12640	0.107	274.8	3.84	0.872	181.510	46.12
3,550	0.428	0.076	3,419.97	11.102%	0.14407	0.115	177.7	4.06	0.608	229.733	48.73
4,186	0.438	0.066	3,286.33	11.102%	0.14407	0.110	239.6	4.29	0.788	229.733	51.53
3,400	0.424	0.080	3,509.50	12.137%	0.15750	0.116	162.3	4.48	0.569	268.262	53.76
3,484	0.436	0.068	3,001.84	12.137%	0.15750	0.115	171.0	4.55	0.513	268.262	54.66
2,950	0.424	0.080	3,157.72	12.834%	0.16655	0.120	113.9	4.73	0.360	291.428	56.77
3,524	0.436	0.067	2,992.45	12.834%	0.16655	0.115	175.0	5.01	0.524	291.428	60.11
2,750	0.419	0.085	3,234.13	13.833%	0.17951	0.122	91.3	5.29	0.295	321.183	63.42
3,495	0.428	0.076	3,373.58	13.833%	0.17951	0.115	172.0	5.56	0.580	321.183	66.75

P	S_o	S_g	GOR	N_p/N	N_p	J	q_o	t	q_g	G_p	t
psi	Fraction	Fraction	SCF/STB	%>	MMSTBO	STB/ D/PSI	STB/D	Years	MMSCF/ D	MMSCF	months
2,730	0.408	0.096	3,695.67	14.809%	0.19218	0.122	89.0	5.84	0.329	354.255	70.06
3,483	0.416	0.087	3,943.65	14.809%	0.19218	0.115	170.9	6.12	0.674	354.255	73.39
2,720	0.393	0.111	4,411.81	15.772%	0.20468	0.122	87.9	6.39	0.388	393.085	76.68
3,421	0.411	0.092	4,156.86	15.772%	0.20468	0.116	164.5	6.67	0.684	393.085	80.02
2,690	0.387	0.116	4,675.54	16.685%	0.21652	0.122	84.4	6.94	0.395	432.032	83.26
3,367	0.406	0.097	4,377.29	16.685%	0.21652	0.116	158.8	7.22	0.695	432.032	86.59
2,650	0.381	0.122	4,967.15	17.570%	0.22801	0.123	79.8	7.49	0.396	471.688	89.88
3,313	0.401	0.102	4,598.74	17.570%	0.22801	0.117	153.1	7.77	0.704	471.688	93.22
2,610	0.375	0.128	5,266.17	18.429%	0.23915	0.123	75.1	8.05	0.396	511.922	96.56
3,261	0.397	0.107	4,821.26	18.429%	0.23915	0.117	147.7	8.32	0.712	511.922	99.89
2,590	0.371	0.133	5,545.14	19.240%	0.24968	0.123	72.8	8.60	0.403	552.082	103.17
3,224	0.392	0.111	5,047.37	19.240%	0.24968	0.117	143.7	8.88	0.725	552.082	106.50
2,570	0.366	0.138	5,845.08	20.024%	0.25985	0.124	70.4	9.15	0.412	592.803	109.75
3,189	0.388	0.116	5,273.23	20.024%	0.25985	0.118	139.9	9.42	0.738	592.803	113.09
2,540	0.360	0.143	6,169.48	20.793%	0.26983	0.124	66.9	9.70	0.413	634.429	116.40

Table 6—Relevant results from gas injection calculations.

Huff-and-Puff Cycle	Remaining Oil-in-Place before injection, N_r	Gas volume in the reservoir, $G_{i+1}^{inj} - G_{pi}^{inj}$	Newton-Raphson Iterations, k
	MMSTB	MMSTB	
1	1.2114	46.4826	6
2	1.1861	41.2945	6
3	1.1713	45.1955	6
4	1.1536	45.6680	6
5	1.1402	39.6298	6
6	1.1311	44.4086	6
7	1.1182	48.0142	6
8	1.1055	51.0289	6
9	1.0930	53.0183	6
10	1.0812	54.9868	6
11	1.0697	56.8290	6
12	1.0586	58.5683	6
13	1.0480	60.3208	6
14	1.0379	61.9732	6

Figure 7 shows the excellent fit for both oil rate and cumulative oil production provided by the MBE equation and the methodology formulated in this paper. It also includes crossplots of gas-oil ratio and average reservoir pressure vs. time. As expected, increasing gas-oil ratios occur once gas injection starts.

Also, the assumption of the average reservoir pressure remaining above the bubble point as injection goes on is corroborated by these results.

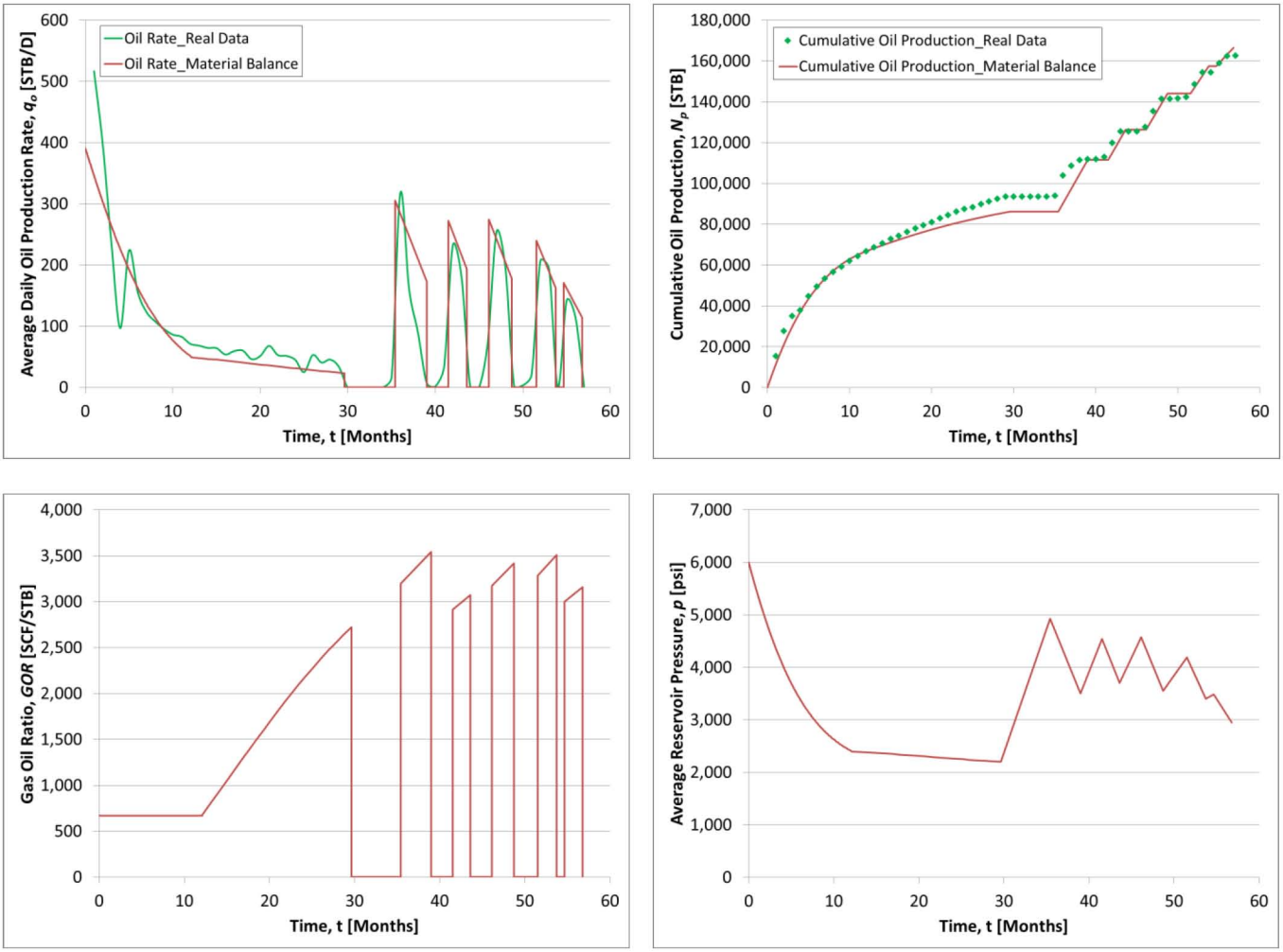

Figure 7—History-matching results for oil rate and cumulative oil production. Also shown are calculated GOR and average reservoir pressure as a function of time.

For production forecasting, gas injection rates of 0.50 MMSCF/D and injection/production times of approximately 100 days/100 days for each huff-and-puff cycle were used. The corresponding plots are presented in Figure 8.

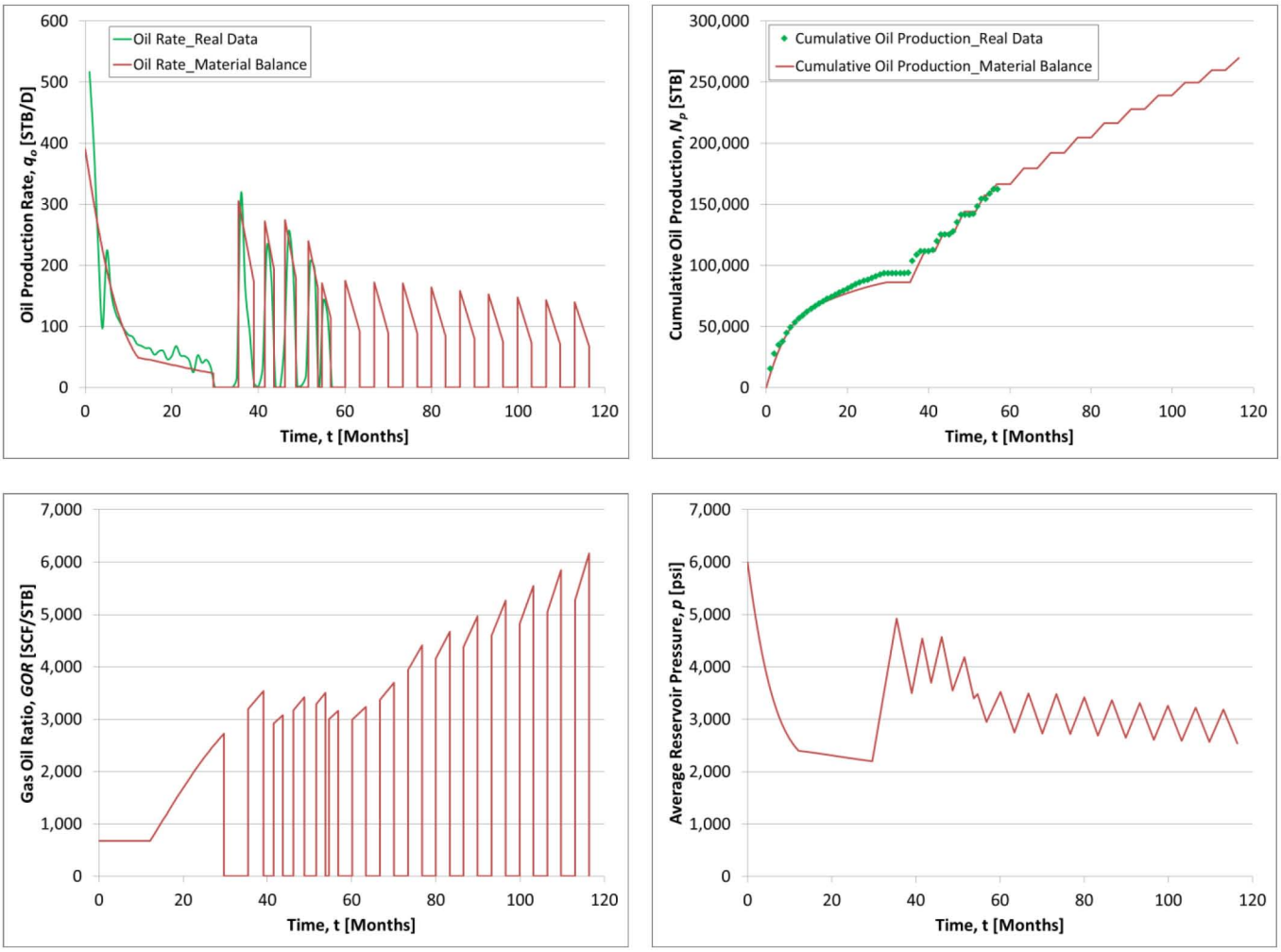

Figure 8—Production forecasting results.

Discussion of Results

Figure 9 shows percent oil recoveries attained by natural depletion over the first 30 months of production and huff-and-puff gas injection over the subsequent 30 months. According to the MBE, 30 months of huff-and-puff gas injection following primary recovery leads to a recovery of about 12.8%. The MBE indicates that primary recovery at the same time would have been in the order 7.4%. Thus, the incremental recovery in 30 months is 5.4%, which is equivalent to 70,075 STB. This results in a significant 73% increase in oil recovery.

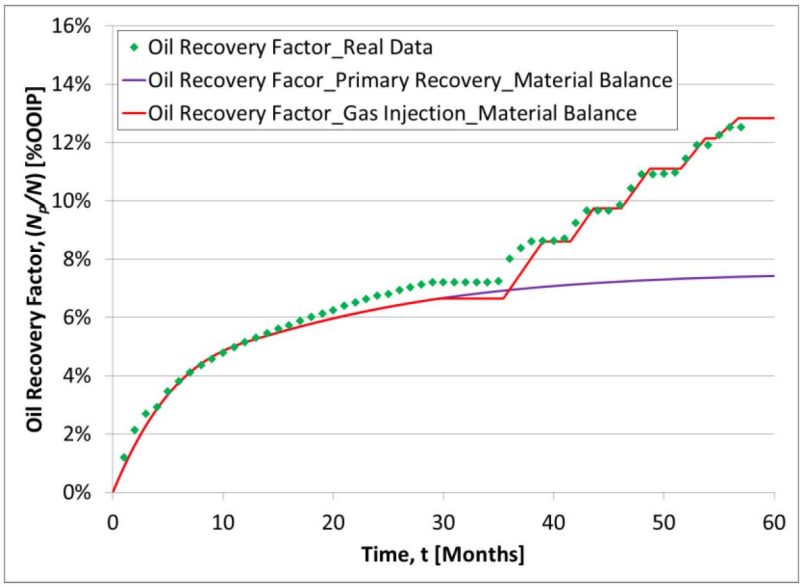

Figure 9—Percent oil recovery over the first 60 months (5 years) of historical and calculated production.

The forecast presented in Figure 10 compares percent oil recoveries after 120 months of production. At 80 months, percent oil recovery by natural depletion becomes flat, and the primary recovery factor after 120 months of production is 7.5%. However, huff-and-puff gas injection yields a recovery of 21%, which corresponds to a very significant 180% increase, or equivalently 175,190 STB. Although the MBE forecast is stopped at 120 months, note that the oil production rates is still over 100 STB/D and the cumulative production is in an increasing path.

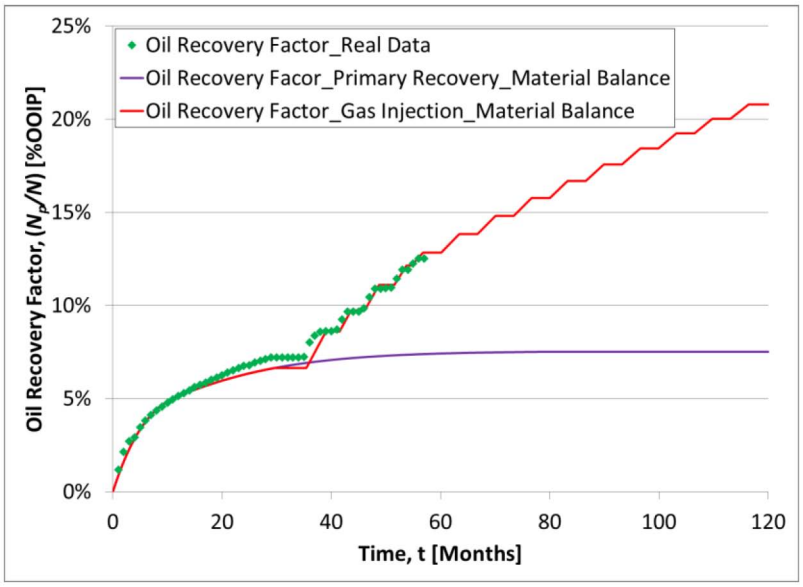

Figure 10—Percent oil recovery over 120 months (10 years) of historical and calculated production.

Results from this pilot demonstrate that recoveries from shale oil reservoirs can be significantly improved by means of huff-and-puff gas injection. Although an economic evaluation is beyond the scope of this paper, the figures presented in this study highlight the promising potential of this IOR technique for boosting oil recoveries in the Eagle Ford shale.

Conclusions

1. A new material balance equation (MBE) to forecast the performance of multiporosity shale oil reservoirs under natural depletion and huff-and-puff gas injection has been developed.
2. Use of the new MBE has been demonstrated with huff-and-puff pilot data of an Eagle Ford shale horizontal well. Results indicate that oil recoveries from shale reservoirs can be significantly improved by means of huff-and-puff gas injection.
3. The new MBE allows making quick and reasonable forecasts of oil rates and cumulative oil production by huff-and-puff gas injection in shale oil reservoirs.
4. Gas containment is a critical aspect for the successful implementation of a huff-and-puff gas injection project in a shale oil reservoir. The concept implies that the injected gas flows into the hydraulic fractures and penetrates the tight matrix, and more importantly, does not escape or leak into adjacent formations.
5. In the pilot study discussed in this paper, gas injection maintains the average reservoir pressure above the bubble point. Thus, the reservoir oil remains undersaturated as long as the huff-and- puff gas injection continues.
6. The iterative Newton-Raphson method exhibits fast convergence for calculating the average reservoir pressure following gas injection.

Acknowledgements

The support of CNOOC Limited, Nexen Energy ULC, Mitacs (through the Mitacs Accelerate Program), the Schulich School of Engineering at the University of Calgary, and Servipetrol Ltd. (Canada) is gratefully acknowledged. We also thank the GFREE research team [GFREE refers to an integrated research program including Geoscience (G); Formation Evaluation (F); Reservoir Drilling, Completion, and Stimulation (R); Reservoir Engineering (RE); and Economics and Externalities (EE)] at the University of Calgary for their continued help and support.

Nomenclature

a	Production decline per year, %
A	Well drainage area, acres
B_g	Gas formation volume factor, vol/vol
B_g^{inj}	Formation volume factor of the injected gas, vol/vol
B_g	Oil formation volume factor, RB/STB
B_{ob}	Oil formation volume factor at bubble point, RB/STB
B_{oi}	Oil formation volume factor at initial reservoir pressure, RCF/SCF
B_{oI}	Oil formation volume factor at p_I, RB/STB
B_w	Water formation volume factor, RB/STB
C	Effective matrix compressibility, psi^{-1}
C"	Effective fracture compressibility, psi^{-1}
C_f	Fracture compressibility, psi^{-1}
C_m	Matrix compressibility, psi^{-1}
C_o	Oil compressibility, psi^{-1}
C_{oe}	Effective oil compressibility, psi^{-1}
C_w	Water compressibility, psi^{-1}
$f(p)$	Linear function for expressing B_o as a function of p
$F(p)$	Function of pressure
$f'(p)$	First derivative of function f

$F'(p)$ First derivative of function F
$g(p)$ Power function for expressing B_g^{inj} as a function of p
$g'(p)$ First derivative of function g
G^{inj} Cumulative gas injection, STB
G_p Cumulative gas production, STB
G_p^{inj} Cumulative gas production from injected gas, STB
h Reservoir thickness, ft
i Subscript denoting pressure step
I_g Continuous gas injection index, fraction
J Productivity index, STB/D/psi
k k-th Newton-Raphson iteration
k_2 Permeability of natural fractures scaled to the bulk volume of the composite system, md
k_{hf} Permeability of hydraulic fractures scaled to the bulk volume of the composite system, md
k_{rg} Relative permeability to gas
k_{rg}^0 Gas relative permeability at residual oil saturation
k_{ro} Relative permeability to condensate
k_{ro}^0 Oil relative permeability at critical gas saturation
L Length of horizontal well, ft
m Size of the gas cap, dimensionless
N Original oil-in-place, STB
N_p Cumulative oil production, STB
N_r Remaining oil-in-place, STB
p Average reservoir pressure, psi
p_{ab} Abandonment pressure, psi
p_i Initial reservoir pressure, psi
P_I Average reservoir pressure before the start of each huff-and-puff cycle, psi
PV Reservoir pore volume, STB
p_{wf} Bottomhole flowing pressure, psi
q_g Gas production rate, MMSCF/D
q_g^{inj} Gas injection rate, MMSCF/D
q_g Oil production rate, STB/D
R Instantaneous gas-oil ratio, SCF/STB
R_{avg} Average gas-oil ratio, SCF/STB
r_{eh} Drainage radius for horizontal well, ft
r_{ev} Drainage radius for vertical well, ft
R_S Gas-oil solution ratio, SCF/SCF
R_{sb} Gas-oil solution ratio at bubble point, SCF/SCF
r_w Wellbore radius, ft
r_w' Effective wellbore radius, ft
S Skin factor
S Normalized saturation, fraction
S_g Gas saturation of the composite system, fraction
S_{gc} Critical gas saturation, fraction
S_o Oil saturation, fraction

S_{of} Oil saturation in fractures, fraction
S_{om} Oil saturation in matrix, fraction
S_{or} Residual oil saturation, fraction
S_w Water saturation, fraction
S_{wf} Water saturation in fractures, fraction
S_{wi} Average initial water saturation of the composite system, fraction
S_{wm} Average water saturation in matrix, fraction
t Time, years
T Reservoir temperature, °R
v Partitioning coefficient, fraction
W_e Cumulative water influx, RB
w_{hf} Hydraulic fracture width, ft
W_p Cumulative water production, STB
x_{hf} Hydraulic fracture half length, ft
Δt^{inj} Duration of injection (huff) period, days

Greek Symbols

Δ Increment between pressure step i and $i+1$ (or $i+1$ and $i+2$)
μ_g Gas viscosity, cp
μ_g^{inj} Viscosity of the injected gas, cp
μ_o Oil viscosity, cp
ϕ_2 Porosity of the fractures system scaled to the bulk volume of the composite system, fraction
ϕ_m Inorganic matrix porosity scaled to the bulk volume of the composite system, fraction
ϕ_{mt} Total matrix porosity, fraction
ϕ_{org} Organic porosity scaled to the bulk volume of the composite system, fraction
ϕ Total shale porosity, fraction
ω Fraction of OOIP stored in fractures, fraction

References

Aguilera, R., 1988. Unsteady State Water Influx in Naturally Fractured Reservoirs. Paper PETSOC- 88-39-64 presented at the Annual Technical Meeting held in Calgary, Alberta, 12 – 16 June 1988.

Aguilera, R., 2006. Effect of Fracture Compressibility on Oil Recovery From Stress-Sensitive Naturally Fractured Reservoirs. *Journal of Canadian Petroleum Technology*, Volume **46**, No. 07, 49 - 59, December 2006. https://doi.org/10.2118/06-12-01.

Aguilera, R., 2007. Effect of Naturally Fractured Aquifers on Oil Recovery From Stress-Sensitive Naturally Fractured Reservoirs. *Journal of Canadian Petroleum Technology*, Volume **46**, No. 07, 43 - 48, July 2007. https://doi.org/10.2118/07-07-04.

Ahmed, T., 2006. *Reservoir Engineering Handbook*, Third Edition. Elsevier. Burlington, MA.

Alharty, N., Teklu, T. W., Kazemi, H., Graves, R. M., Hawthorne, S. B., Braunberger, J., and Kurtoglu, B., 2017. Enhanced Oil Recovery in Liquid-Rich Shale Reservoirs: Laboratory to Field. *In press: SPE Journal of Reservoir Evaluation and Engineering*. https://doi.org/10.2118/175034-PA.

Chapra, S. and Canale, R., 2009. *Numerical Methods for Engineers with Personal Computer Applications*, Fifth Edition. McGraw Hill. New York, NY.

Craft, B. C., and Hawkins, M. F., 1959. *Applied Petroleum Reservoir Engineering*. Prentice-Hall Inc. Englewood Cliffs, NJ.

Egboga, N. U., Mohantym K. K., and Balhoff, M. T., 2017. A Feasibility Study of Thermal Stimulation in Unconventional Shale Reservoirs. *Journal of Petroleum Science and Engineering*, Volume **154**, 576 - 588, June 2017. https://doi.org/10.1016/j.petrol.2016.10.041.

Fragoso, A., 2016. *Improving Recovery of Liquids from Shales Through Gas Injection*. MSc thesis, Department of Chemical and Petroleum Engineering, University of Calgary.

Fragoso, A., Trick, M., Harding, T., Selvan, K., and Aguilera, R., 2018a. Coupling of Wellbore and Surface Facilities Models with Reservoir Simulation to Optimize Recovery of Liquids from Shale Reservoirs. SPE Paper 185079 presented at the SPE Unconventional Resources Conference held in Calgary, Alberta, Canada, 15 – 16 February 2017. In press: SPE Journal of Reservoir Evaluation and Engineering, 2018.

Fragoso, A., Aguilera, R., and Selvan, K., 2018b. Breaking a Paradigm: Can Oil Recovery From Shales Be Larger Than Oil Recovery From Conventional Reservoirs? The Answer Is Yes! SPE Paper 189784 presented at the SPE Canada Unconventional Resources Conference held in Calgary, Alberta, Canada, 13 – 14 March 2018.

Gamadi, T. D., Elldakli, D., and Sheng J. J., 2014. Compositional Simulation Evaluation of EOR Potential in Shale Oil Reservoirs by Cyclic Natural Gas Injection. URTeC paper 1922690 presented at the Unconventional Resources Technology Conference held in Denver, Colorado, USA, 25 – 27 August 2014.

Hartmann, D. J., and Beaumont, E. A., (1999). Predicting Reservoir System Quality and Performance. In *Exploring for Oil and Gas Traps, AAPG Treatise of Petroleum Geology, Handbook of Petroleum Geology*, ed. Edward A. Beaumont and Norman H. Foster, pp. 9-1 - 9-154.

Hoffman, B. T., and Evans, J. G., 2016. Improved Oil Recovery IOR Pilot Projects in the Bakken Formation. SPE Paper 180270 presented at the SPE Low Perm Symposium held in Denver, Colorado, USA, 5 – 6 May 2016.

Hubbert, M. K., and Willis, D. G., 1957. Mechanics of Hydraulic Fracturing. *American Institute of Mining, Metallurgical, and Petroleum Engineers*, Volume **210**, 153 - 168, 1957.

Jacobs, T. 2016. EOR for Shale: Ideas to Boost Output Gain Traction. *Journal of Canadian Petroleum Technology*, Volume **68**, No. 06, 28 - 31, June 2016. https://doi.org/10.2118/0616-0028-JPT.

Joshi, S., 1991. *Horizontal Well Technology*. PennWell Books. Tulsa, OK.

Orozco, D., 2016. *A New Material Balance Methodology for Quintuple Porosity Shale Gas and Shale Condensate Reservoirs*. MSc Thesis, Department of Chemical and Petroleum Engineering, University of Calgary.

Railroad Commission of Texas, 2017. *Eagle Ford Shale Information*. http://www.rrc.state.tx.us/oil-gas/major-oil-and-gas-formations/eagle-ford-shale-information/ (accessed 10 December 2017).

Ramirez, J., and Aguilera, R., 2016. Factors Controlling Fluid Migration and Distribution in the Eagle Ford Shale. *SPE Journal of Reservoir Evaluation and Engineering*, Volume **19**, No. 03, 403 - 414. http://dx.doi.org/10.2118/171626-PA.

Rassenfoss, S., 2017a. Stress About Production? Consider a Chemical Cocktail. *Journal of Petroleum Technology*, Volume **69**, No. 12, December 2017.

Rassenfoss, S., 2017b. Shale EOR Works, But Will It Make a Difference? *Journal of Petroleum Technology*, Volume **69**, No. 10, 34 - 40, October 2017. https://doi.org/10.2118/1017-0034-JPT.